Proceedings of the 2nd International Symposium
on Adaptive Motion of Animals and Machines,
Kyoto, March.4-8, 2003

Analysis of Dynamics of Passive Walking from Energy Function and Eigenvalues

Yoshito Ikemata, Akihito Sano and Hideo Fujimoto
Department of Mechanical Engineering
Nagoya Institute of Technology
Gokiso-cho, Showa-ku, Nagoya 466-8555 JAPAN
{ikemata, sano, fujimoto}@vier.mech.nitech.ac.jp

Abstract

It is well known that passive walking robot can dynamically walk down with a steady gait by only powered gravity. The dynamics of passive walking has interesting characteristics of stability and bifurcation. Since passive gait is natural motion, investigation of passive walking may lead us to understand human locomotion and design for active walking robot.

In this paper, the dynamics of passive walking is investigated from the aspect of energy function. We demonstrate the relationship between the limit cycle area and the rate of energy supplied by potential energy. Also, analysis of eigenvalues reveals the behavior of local stability and mechanism of bifurcation.

1. Introduction

The bipedal walking is central aspect of human behavior in human motion. Human motion is controlled by the nervous system and powered by muscle. Furusho and Sano[1] achieved smooth 3D walking through control based on information obtained from a variety of sensors. However, McGeer[2] demonstrated that biped robot can walk a gentle slope with no energy source other than gravity and no control. This motion is attractive because its gait is natural. McGeer's result suggests that the dynamics of passive walking inherently generates gait cycle. The study of passive walking may yield insight into human locomotion and the design of humanoid robot.

Many researchers have studied this category of biped robot. Goswami et al.[3][4] and Garcia et al.[5] studied numerically the passive gait and verified the symmetric and chaotic motion. Osuka et al.[6] demonstrated the stability and chaotic characteristics of passive walking by the real robot. Collins et al.[7] demonstrated the 3-D passive walking is possible. Asano et al.[8] proposed the control of biped walking robot based on passive walking. The dynamics of passive walking has been studied by many researchers. However, the mechanisms of limit cycle and bifurcation are not well understood.

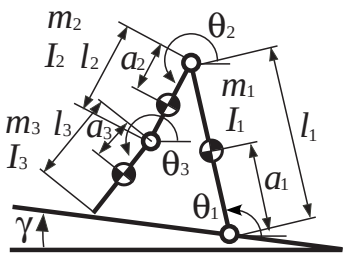

Figure 1: Kneed biped model

In this paper, we analyze the dynamics of passive walking from the walking robot's energy and the rate of change of this energy. In addition, we focus the features of dynamics which the kneed and straight-legged walkers have in common. The straight-legged walker is same as kneed walker with locked knees of both legs. These features may be the essence of passive walking. And behavior of stability of fixed point is investigated by analysis of eigenvalues.

2. Passive Walking

2.1. Kneed Biped Model

Figure 1 shows the model of kneed biped robot. This model consists of stance leg and swing leg, connected by a frictionless joint at the hip. Each leg has thigh and shank. The stance knee is locked. The swing knee is a frictionless joint with a knee-stop. Initial conditions are that both legs are straight and touch the ground. The equations of

motion for the three-link mode can be written as

$$\boldsymbol{M}(\boldsymbol{\theta})\ddot{\boldsymbol{\theta}} + \boldsymbol{N}(\boldsymbol{\theta}, \dot{\boldsymbol{\theta}})\dot{\boldsymbol{\theta}} + \boldsymbol{G}(\boldsymbol{\theta}) = \boldsymbol{\tau} \tag{1}$$

where $\boldsymbol{M}$ is the 3×3 inertia matrix, $\boldsymbol{N}(\boldsymbol{\theta}, \dot{\boldsymbol{\theta}})$ is the 3×3 colioris matrix, $\boldsymbol{G}(\boldsymbol{\theta})$ is the 3×1 gravity matrix. $\boldsymbol{\tau}$ is the vector of joint torque. Also, $\boldsymbol{\theta}(= [\theta_1, \theta_2, \theta_3]^T)$ is the vector of joint angles. In this paper, we deal with a passive walking where $\boldsymbol{\tau} = \boldsymbol{0}$. Knee-strike occurs when the swing leg becomes straight. The swing knee locks instantaneously, and the swing leg remains straight thereafter. This state can be regarded as that of compass-like biped robot. We applied the following transition rule when the swing foot hits the ground. The stance leg leaves the ground at the instant when the swing leg contacts the ground. For an inelastic no-sliding collision with the ground, the robot's angular momentum just before and just after its collision[9] is conserved. By using the conservation of angular momentum principle, the relation $\boldsymbol{Q}^- \dot{\boldsymbol{\theta}}^- = \boldsymbol{Q}^+ \dot{\boldsymbol{\theta}}^+$ can be deriven, where the"+" superscript means "just after the collision" and the "–" superscript means "just before the collision". The joint-velocity just after collision can be given as

$$\dot{\boldsymbol{\theta}}^+ = (\boldsymbol{Q}(\alpha)^+)^{-1}\boldsymbol{Q}(\alpha)^- \dot{\boldsymbol{\theta}}^- = \boldsymbol{H}(\alpha)\dot{\boldsymbol{\theta}}^- \tag{2}$$

where $\boldsymbol{H}(\alpha)$ is the 2×2 matrix. α is the inter-leg angle at heel-strike. In this paper, the physical parameters are set as shown in Table 1.

Table 1: Notations and numerical settings

m_1	Stance leg mass	5[kg]
m_2	Thigh mass	2.5[kg]
m_3	Shank mass	2.5[kg]
l_1	Stance leg length	0.7[m]
l_2	Thigh length	0.35[m]
l_3	Shank length	0.35[m]
a_1	Lower part of stance leg	0.35[m]
a_2	Lower part of thigh	0.175[m]
a_3	Lower part of shank	0.175[m]
I_1	Moment of inertia of stance leg about its ceter of gravity	0.2041[kgm^2]
I_2	Moment of inertia of thigh	0.0255[kgm^2]
I_3	Moment of inertia of shank	0.0255[kgm^2]
γ	Slope angle	
θ_1	Stance leg angle	
θ_2	Thigh angle	
θ_3	Shank angle	
α	Inter-leg angle at heel-strike	

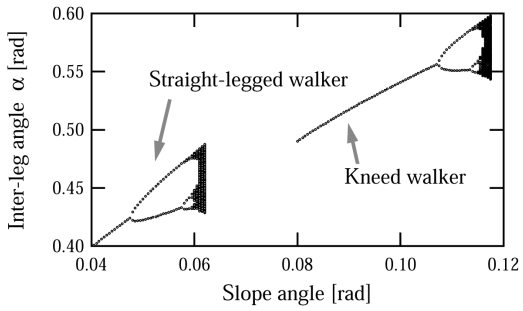

(a) Inter-leg angle

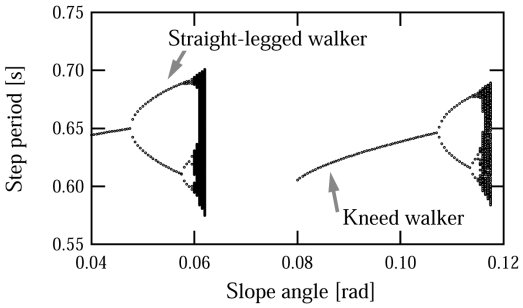

(b) Step period

Figure 2: Period doubling route to chaos in stable kneed and straight-legged walking motions

2.2. Bifurcation

The kneed and straight-legged walkers can exhibit period doubling and chaos gait as shown in Fig.2. The straight-legged walker is same as kneed walker with locked knees of both legs. At the bifurcation point, the inter-leg angle α of kneed walker is larger than that of straight-legged walker. However, it is interesting that the step period of kneed walker is nearly equal to that of straight-legged walker.

3. Energy Function

3.1. Storage Energy

One cycle is defined as the period from the state just after heel-strike to the next same state. In one cycle, the energy supplied by potential energy for walking down is expressed as ΔE_p. The energy lost by knee-lock and heel-strike are expressed as ΔE_{lk} and ΔE_{lh} respectively. The storage energy of the walker can be defined as follows:

$$\Delta E_s = \Delta E_p - \Delta E_{lk} - \Delta E_{lh} \tag{3}$$

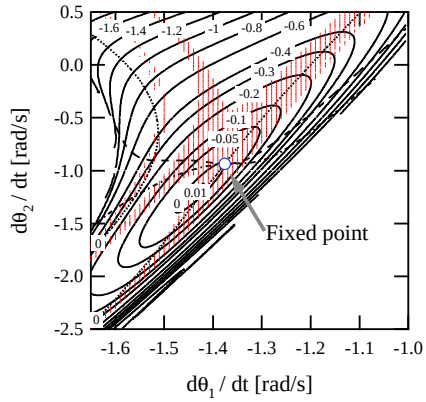

(a) Straight-legged walker

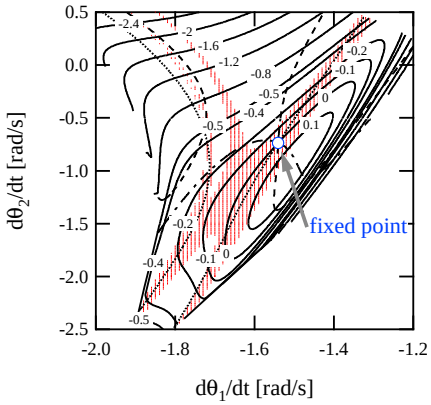

(b) Kneed walker

Figure 3: Storage energy ΔE_s before bifurcation

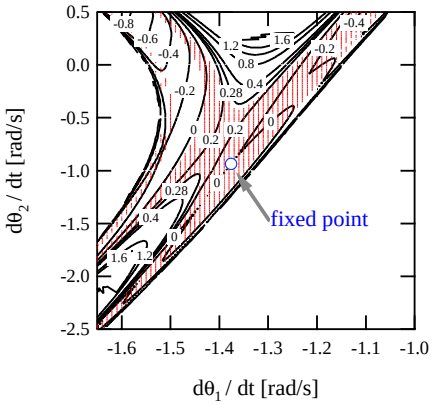

(a) Straight-legged walker

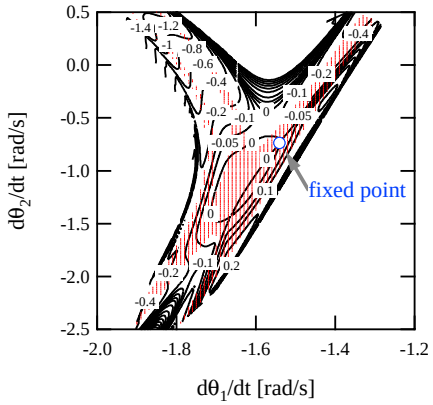

(b) Kneed walker

Figure 4: Supply rate ΔE_{rs} before bifurcation

In a stable 1-periodic gait, the storage energy becomes $\Delta E_s = 0$. It is very difficult to derive analytically the storage energy, since the walker has nonlinear dynamics and the time of heel-strike can not be given explicitly. The storage energy is numerically calculated in the condition that the inter-leg angle is fixed.

Figure 3 shows the contour of the storage energy of straight-legged walker and kneed walker in case of slope angle γ=0.045, 0.106[rad] (before bifurcation) and inter-leg angle α=0.4161420, 0.5540910[rad] (at stable gait) respectively. The horizontal and vertical axes denote the angular velocities of stance leg and swing leg respectively. The dotted line, the dashed line, the dashed and dot line represent that α, $\dot{\theta}_1$, $\dot{\theta}_2$ are equal to those after one cycle respectively. A cross-point of these three lines is equivalent to fixed point.

The shape of ΔE_s is gradual convexity and its contour looks like the distorted ellipse. It is unexpected that the fixed point is located in the boundary line between positive and negative rather than in the top or bottom of the contour ΔE_s. The area in which the ΔE_s is positive is limited. This means that the energy supplied by potential energy is larger than the energy loss. In addition, the area that the walker is absorbed in the limit cycle which is derived from simulation is overlaid as the shaded area. The dotted line is almost included in area of limit cycle.

3.2. Supply Rate

The supply rate is defined as follows:

$$\Delta E_{rs} = \frac{|\Delta E_{s2}| - |\Delta E_{s1}|}{\Delta 1 cycle} \tag{4}$$

where ΔE_{s1} and ΔE_{s2} are two consecutive storage energies. ΔE_{rs} is equal to 0 at a stable 1-periodic gait. Supply rate ΔE_{rs} is negative when the system approaches the limit cycle. However, $\Delta E_{rs} < 0$ doesn't indicate that the system always is absorbed in limit cycle. Figure 4 shows the supply rate ΔE_{rs} for the same conditions as Fig.3.

As compared with Fig.3, it notes that the applicable area is reduced, since two successful steps are required. In case of straight-legged walker, the boundary of the limit cycle area seems to correspond to the contour of ΔE_{rs}. While, in case of kneed walker, there is no such relation.

Then, we focus on the energy supplied by potential energy ΔE_p composed in the supply rate ΔE_{rs}. The rate of change of energy supplied by potential energy ΔE_{rp} can be written as

$$\Delta E_{rp} = \frac{|\Delta E_{p2}| - |\Delta E_{p1}|}{\Delta 1 cycle} \tag{5}$$

Figure 5 shows the rate of energy supplied ΔE_{rp}. Both walkers have the relation between the contour of ΔE_{rp} and the boundary of limit cycle area. Furthermore, it is interesting to note that the values of this contour of both walkers are same, $\Delta E_{rp} = -0.5$. This feature may be useful to predict whether the system can be absorbed in limit cycle.

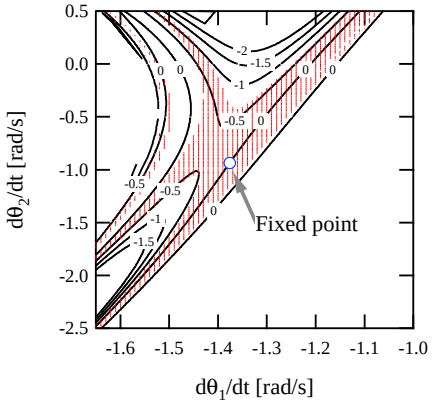

(a) Straight-legged walker

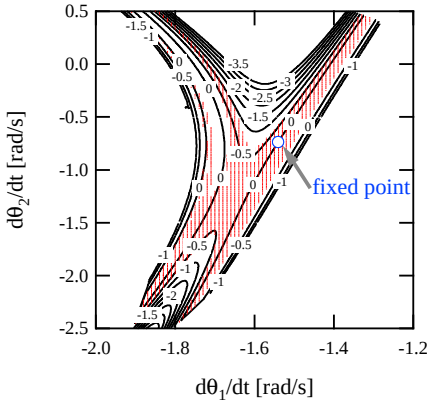

(b) Kneed walker

Figure 5: Rate of change of energy supplied by potential energy ΔE_{rp}

In figure 4, the negative area of ΔE_{rs} around the fixed point is very narrow. Figure 6 shows the supply rate around the fixed point. The horizontal and vertical axes denote the angular velocities of stance leg and inter-leg angle respectively. The angular velocity of swing leg is assumed as $\dot{\theta}_2 = k_1\dot{\theta}_1 + k_2$, since the state just after heel-strike near the limit cycle approaches the fixed point linearly. The states just after heel-strike at every step are overwritten as circle mark. In both kneed and straight leg walkers, the state approaches the fixed point linearly visiting the two subarea of $\Delta E_{rs} < 0$.

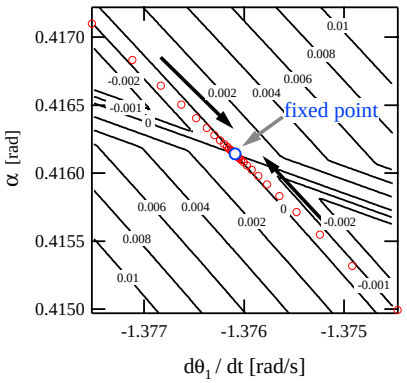

(a) Straight-legged walker

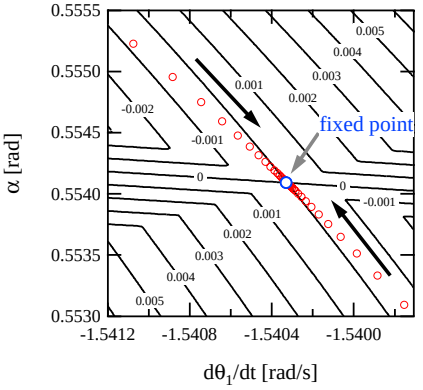

(b) Kneed walker

Figure 6: Supply rate around fixed point

3.3. Supply Rate after Bifurcation

If 1-perodic gait exists, the cross point exist as same as shown in Fig.3. We investigated the existence of the cross point in case of slope angle leading to 2-periodic gait, γ=0.050[rad] for straight-legged walker and γ=0.110[rad] for kneed walker. As a result, the cross-point occurs when inter-leg angle is set to α=0.4321466, 0.5625966[rad] respec-

tively. Figure 7 shows the supply rate around fixed point. The state gets away from the fixed point linearly through the area of positive supply rate. This result indicates that the fixed point is unstable.

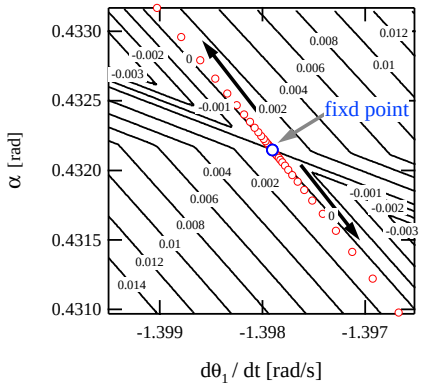

(a) Straight-legged walker

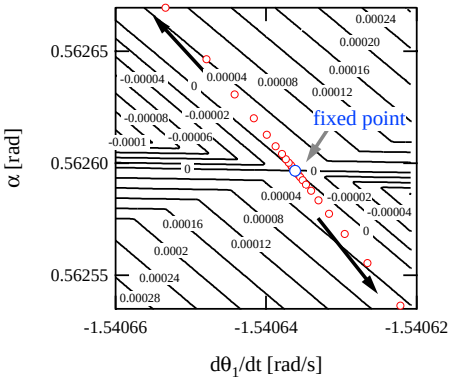

(b) Kneed walker

Figure 7: Supply rate around fixed point after bifurcation

4. Local Stability and Bifurcation

4.1. Eigenvalues and Behavior of Fixed Point

The state just after heel-strike can be expressed as $\boldsymbol{x} = [\alpha\ \dot{\theta}_1\ \dot{\theta}_2]^T$. Successive states of the robot can be related as

$$\boldsymbol{x}_{k+1} = \boldsymbol{f}(\boldsymbol{x}_k) \tag{6}$$

$\boldsymbol{x}^*$ such that $\boldsymbol{x}^* = \boldsymbol{f}(\boldsymbol{x}^*)$ is called the fixed point of the mapping. For a small perturbation $\Delta\boldsymbol{x}^*$ around the limit cycle, the nonlinear mapping function $\boldsymbol{f}$ can be expressed in terms of Taylor series expansion as

$$\boldsymbol{x}_{k+1} = f(\boldsymbol{x}^*) + \frac{\partial f}{\partial \boldsymbol{x}}\Big|_{\boldsymbol{x}=\boldsymbol{x}^*}\Delta\boldsymbol{x}_k \tag{7}$$

From Eq.(7) and $\boldsymbol{x}^* = \boldsymbol{f}(\boldsymbol{x}^*)$, linear difference equation can be obtained as follow:

$$\Delta\boldsymbol{x}_{k+1} = \frac{\partial f}{\partial \boldsymbol{x}}\Big|_{\boldsymbol{x}=\boldsymbol{x}^*}\Delta\boldsymbol{x}_k \equiv \boldsymbol{J}\Delta\boldsymbol{x}_k \tag{8}$$

where $\boldsymbol{J}$ is the gradient of f with respect to state variables. The vector of eigenvalues of $\boldsymbol{J}$ at the fixed point $\boldsymbol{x}^*$ is presented by $\boldsymbol{\lambda}$. If $\boldsymbol{\lambda}$ doesn't have multiple root, the general solution of Eq.(8) can be written as

$$\Delta\boldsymbol{x}_k = \sum_{i=1}^{3} c_i\lambda_i^k\boldsymbol{v}_i \tag{9}$$

Where c_i is constant and $\boldsymbol{v}_i$ is eigenvector associated with eigenvalue λ_i. The stability and behaviors of fixed point are followings:

(a1) If all $|\lambda_i| < 1$, the fixed point is *sink*-type and stable.

(a2) If at least one of $|\lambda_i| < 1$ and the others $|\lambda_i| > 1$, it is *saddle*-type and unstable.

(a3) If all $|\lambda_i| > 1$, it is *source*-type and unstable.

4.2. Analysis of Eigenvalues

It is very difficult to calculate the matrix $\boldsymbol{J}$. Eq.(7) can be rewritten as

$$\begin{aligned}\boldsymbol{J}\Delta\boldsymbol{x}^* &= f(\boldsymbol{x}^* + \Delta\boldsymbol{x}) - f(\boldsymbol{x}^*) \\ &= f(\boldsymbol{x}^* + \Delta\boldsymbol{x}) - \boldsymbol{x}^*\end{aligned} \tag{10}$$

where $\boldsymbol{f}(\boldsymbol{x}^* + \Delta\boldsymbol{x}^*)$ is the first return map of the perturbed state $\boldsymbol{x}^* + \Delta\boldsymbol{x}^*$. As it is not practical to analytically calculate the matrix $\boldsymbol{J}$, we do so numerically[3].

Figure 8 shows loci of eigenvalues of the matrix $\boldsymbol{J}$ with slope angles γ. When the slope angle increases, one of the eigenvalues approaches origin along the real axis. The other two, move along the real axis to a certain point, then along elliptic orbit to another point on the real axis. From there, again along the real axis, one of the eigenvalues approaches the origin, while the other moves away from it. At slope angle γ=0.050[rad] for the straight-legged walker and γ=0.110[rad] for the kneed walker, one of the eigenvalues is outside the unit circle. This means that this fixed point is saddle-type and unstable. This result corresponds to the feature as mentioned in Section 3.3. Consequently, the stable fixed point becomes unstable at slope angle leading to bifurcate periodic gait.

Also, unstable 1-periodic gait may be able to be stabilized if the eigenvalue is moved in the unit circle by the controller.

In figure 8(b), one of the eigenvalues likely will be outside the unit circle with the slope angle less than about 0.079[rad]. This result is in agreement with the feature in Fig.2.

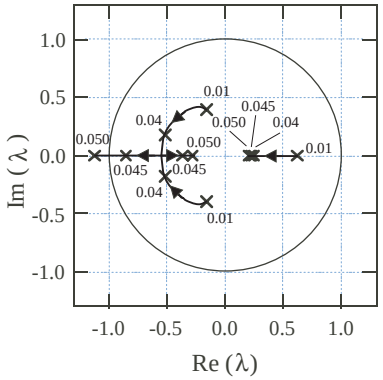

(a) Straight-legged walker

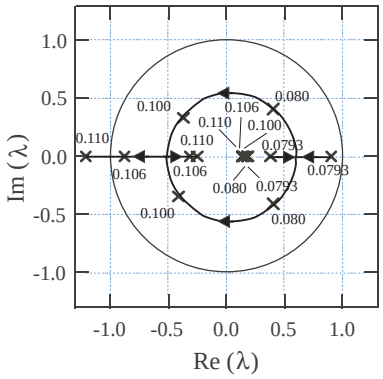

(b) Kneed walker

Figure 8: Loci of eigenvalues of $\boldsymbol{J}$

5. Conclusions

In this paper, we investigated the passive-dynamics of kneed and straight-legged walker from the aspect of walker's energy and eigenvalues. The results of this paper are summarized as follows:

1. Area of storage energy that is positive is limited. This indicates that energy supplied by potential energy almost become smaller than energy loss. The line representing the inter-leg angle is the same for next step is almost included in area of the limit cycle.

2. The contour of the rate of energy supplied by potential energy has relevance to the boundary of the limit cycle area. Potential energy depends only on the inter-leg angle at heel-strike. It may be able to estimating whether to be absorbed in limit cycle from the rate of inter-leg angle at heel-strike.

3. The eigenvalues with slopes were analyzed. For large slope angle, one of the eigenvalues is outside the unit circle. This means that the fixed point is unstable. As a result, the periodic gait bifurcates. There is a possibility of stabilizing a unstable gait if the eigenvalue can be moved in the unit circle by the controller.

References

[1] J. Furusho and A. Sano: "Sensor-Based Control of a Nine-Link Biped, " *The Int. J. of Robotics Research*, Vol.9, No.2, pp.83–98, 1990.

[2] T. McGeer: "Passive Dynamic Walking, " *The Int. J. of Robotics Research*, Vol.9, No.2 pp.62–82, 1990.

[3] A. Goswami, B. Thuilot and B. Espau: "Compass-like Biped Robot Part I : Stability and Bifurcation of Passive Gaits, " *Technical Report 2996 INRIA*, 1996.

[4] A. Goswami, B. Thuilot and B. Espau: "A Study of the Passive Gait of a Compass-Like Biped Robot : Symmetry and Chaos, " *The Int. J. of Robotics Research*, Vol.17, No.12, pp.1282–1301, 1998.

[5] M. Garcia, A. Chatterjee, A. Ruina and M. Coleman: "The Simplest Walking Model : Stability, Complexity, and Scaling, " *J. of Biomechanical Engineering*, Vol.120, pp.281–288, 1998.

[6] K. Osuka and K. Kirihara: "Motion Analysis and Experiments of Passive Walking Robot QUARTET II, " *Proc. of the 2000 IEEE Int. Conf. on Robotics & Automation*, pp.3052–3056, 2000.

[7] S. H. Collins, M. Wisse, and A. Ruina: "A Three-Dimensional Passive-Dynamic Walking Robot with Two Legs and Knees, " *The Int. J. of Robotics Research*, Vol.20, No.7, pp.607–615, 2001.

[8] F. Asano, M. Yamakita and K. Furuta: "Virtual Passive Dynamic Walking and Energy-based Control Laws, " *Proc. of the 2000 IEEE/RSJ Int. Conf. on Intelligent Robots and Systems*, pp.1149–1154, 2000.

[9] Y. Hurmuzlu, T. Chang: "Rigid Body Collisions of a Special Class of Planar Kinematic Chains, " *IEEE Trans. on Systems, Man, Cybernetics*, Vol. 22, No. 5 pp.964–971, 1992.